Cell

The 3D Structure of the Immunoglobulin Heavy-Chain Locus: Implications for Long-Range Genomic Interactions

Suchit Jhunjhunwala,[1,7] Menno C. van Zelm,[1,7] Mandy M. Peak,[1,7] Steve Cutchin,[2] Roy Riblet,[3] Jacques J.M. van Dongen,[4] Frank G. Grosveld,[5] Tobias A. Knoch,[5,6,*] and Cornelis Murre[1,*]
[1]Division of Biological Sciences, 0377, University of California, San Diego, La Jolla, CA 92093, USA
[2]San Diego Supercomputer Center, University of California, San Diego, La Jolla, CA 92037, USA
[3]Torrey Pines Institute for Molecular Studies, San Diego, CA 92121, USA
[4]Department of Immunology
[5]Departments of Biophysical Genomics, Cell Biology and Genetics
Erasmus MC, Dr. Molewaterplein 50, 3015 GE Rotterdam, The Netherlands
[6]Ruperto-Carola University Heidelberg, Kirchhoff Institute for Physics, Department of Biophysical Genomics,
Im Neuenheimfer Feld 280, 69120 Heidelberg, Germany
[7]These authors contributed equally to this work.
*Correspondence: ta.knoch@taknoch.org (T.A.K.), murre@biomail.ucsd.edu (C.M.)
DOI 10.1016/j.cell.2008.03.024

SUMMARY

The immunoglobulin heavy-chain (*Igh*) locus is organized into distinct regions that contain multiple variable (V_H), diversity (D_H), joining (J_H) and constant (C_H) coding elements. How the *Igh* locus is structured in 3D space is unknown. To probe the topography of the *Igh* locus, spatial distance distributions were determined between 12 genomic markers that span the entire *Igh* locus. Comparison of the distance distributions to computer simulations of alternative chromatin arrangements predicted that the *Igh* locus is organized into compartments containing clusters of loops separated by linkers. Trilateration and triple-point angle measurements indicated the mean relative 3D positions of the V_H, D_H, J_H, and C_H elements, showed compartmentalization and striking conformational changes involving V_H and D_H-J_H elements during early B cell development. In pro-B cells, the entire repertoire of V_H regions (2 Mbp) appeared to have merged and juxtaposed to the D_H elements, mechanistically permitting long-range genomic interactions to occur with relatively high frequency.

INTRODUCTION

It is well-established that higher order chromatin organization plays a pivotal role in genome function (Cremer and Cremer, 2001). For more than a century, the organization of chromosomes and its functional implications in eukaryotes have been extensively studied using light microscopy (Rabl, 1885; Bover, 1909). Electron micrographs of chromosome spreads have suggested the presence of loops, with sizes of ~90 kbp, that interact with a postulated nuclear matrix and aggregate during mitosis into rosettes containing ~18 loops, resulting in ~100 rosettes per average chromosome (Paulson and Laemmli, 1977; Paulson, 1988; Pienta and Coffey, 1984). Similar rosette-like structures have been detected in interphase cells (Okada and Commings, 1979).

As a first approach to resolving chromosome conformation, fluorescence in situ hybridization studies, measuring spatial distances in interphase nuclei between genomic markers as a function of genomic separation, suggested a random walk behavior (Trask et al., 1991). However, confinement of chromosome arms and bands to territories indicated the presence of spatial constraints. More recent observations showed that the spatial distance depends on the genomic distance according to a power law with exponents of 0.5 below and 0.32 above a genomic separation of 4 Mbp (Trask et al., 1993; Warrington and Bengtsson, 1994; Sachs et al., 1995; Münkel and Langowski, 1998). The constraints and the scaling behavior suggested a Random-Walk/Giant-Loop (RW/GL) configuration (Sachs et al., 1995; Yokota et al., 1995). In the RW/GL model, the 30 nm fiber forms 2 to 5 Mbp loops that are attached to a polymer backbone. The backbone and the chromatin fiber within the loops follow random walk dynamics. However, distance measurements between genetic markers with genomic separations of less than 4 Mbp were incompatible with the RW/GL model, but were consistent with another topology, named the Multi-Loop-Subcompartment (MLS) model (Münkel and Langowski, 1998; Knoch, 2002). The MLS model proposes that the 30 nm fiber is folded into rosettes of small loops, connected by linkers of variable sizes.

Recently computer models have been developed to evaluate and test experimental results, designs and hypotheses about the three-dimensional genome organization (Knoch et al., 2000; Knoch, 2002). Beyond supporting the chromatin organization into chromosome territory, arm and band domains, these simulations may reveal how the local, global and dynamic characteristics of cell nuclei are inter-connected (Knoch et al., 2000; Knoch, 2002).

How genes are regulated by spatial rearrangement has been a topic of intensive study. In prokaryotes, transcriptional

enhancers act through looping or tracking along the intervening DNA (Herendeen et al., 1992; Rombel et al., 1998). In eukaryotic cells, chromatin compaction and looping, the presence of DNase I hypersensitive sites at regulatory elements, including transcriptional enhancers, insulators and locus control regions, influence gene expression over large genomic distances (Banerji et al., 1981). The globin locus control region was shown to act over a large distance by looping the intervening region and physically associating with actively transcribing β-globin genes (Carter et al., 2002; Tolhuis et al., 2002). Other loci also have been shown to bring distant enhancer elements into proximity of promoter regions by looping, including the Th2 cytokine locus and the interferon gamma gene (Spilianakis and Flavell, 2004; Eivazova and Aune, 2004).

The murine immunoglobulin heavy-chain locus (*Igh*), spanning 3 Mbp, is organized into distinct segments encoding the variable (V_H), diversity (D_H), joining (J_H), and constant (C_H) regions. Eight constant regions encode the various isotypes, C_μ, C_δ, $C_{\gamma 1}$ $C_{\gamma 2a}$, $C_{\gamma 2b}$, $C_{\gamma 3}$, C_α, and C_ε. Twelve D_H and four J_H segments are positioned immediately upstream of the C_μ region. There are approximately 100 functional V_H gene segments that belong to fifteen partially interspersed families (Brodeur and Riblet, 1984). The V_H, D_H and J_H coding elements are each flanked by recombination signal sequences (RSSs) that act as recognition elements for the V(D)J-recombinase, comprised of RAG1 and RAG2 (Schatz and Spanopoulou, 2005; Jung et al., 2006).

The Ig heavy- and Ig light-chain genes undergo ordered rearrangement during B-lineage development (Alt et al., 1984). In pro-B cells, D_H to J_H rearrangement precedes V_H to D_HJ_H joining. Once an in-frame V(D)J joint has been generated, a pre-B cell receptor is formed, suppressing RAG1/2 activity, and preventing continued *Igh* gene rearrangement. Fluorescence in situ hybridization analysis has demonstrated that in B-lineage cells, the *Igh* locus undergoes substantial contraction and looping (Kosak et al., 2002; Fuxa et al., 2004; Roldan et al., 2005; Sayegh et al., 2005). Despite these observations, how the *Igh* chromatin fiber is organized in 3D space prior to the onset of DNA recombination remains to be resolved. Here, we have used spectral high precision epifluorescence microscopy to determine spatial distance distributions between 12 genomic markers that span the entire *Igh* locus. These data were analyzed to provide a statistical description of the *Igh* locus architecture.

In summary, the data revealed the average relative 3D positions of the V_H, D_H, J_H and C_H elements, indicated the presence of chromatin territories and showed striking conformational changes in *Igh* topology during early B cell development. In pro-B cells, the entire repertoire of V_H elements (2 Mbp) seemed to have merged to be positioned in close proximity to the D_H elements, mechanistically permitting long-range genomic interactions to occur with relatively high frequency.

RESULTS

Methodology for High-Resolution Spatial Distance Measurements between Genomic Markers in B-lineage Cells

To determine the 3D architecture of the *Igh* locus, the spatial distances separating multiple markers located throughout the locus were measured as described previously (Solovei et al., 2002; Sayegh et al., 2005). Two cell types were used in these studies: (1) E2A-deficient pre-pro-B cells were examined, since these cells are arrested at the pre-pro-B cell stage and have not yet committed to the B cell lineage (Ikawa et al., 2004). (2) RAG2-deficient pro-B cells were chosen since they are committed to the B cell lineage but, unlike wild-type pro-B cells, carry the *Igh* locus in germ-line configuration (Shinkai et al., 1992). Pre-pro-B cells and pro-B cells were fixed, permeabilized and hybridized with two 10 kbp probes and a BAC probe, located 3′ of the *Igh* locus (Figure 1A and Figure S1 available online). Although the intensity varied, the fluorescent signals emitted by the 10 kbp probes were clearly detectable (Figure S1). The effective resolution ('Resolution equivalent', see supplemental materials and methods) we obtained using two different colors ranged from 35 to 47 nm for the different combinations of the fluorochromes (Tables S1 and S2). Thus, this approach allowed us to measure spatial distances with a 3D resolution better than 50 nm.

3D Architecture of the Immunoglobulin Heavy-Chain Locus

To dissect the topology of the *Igh* locus, spatial distances were measured between an anchor, BAC probe RP23-201H14, which served as a marker located down-stream of the *Igh* locus and eleven 10 kbp probes that span the entire locus (Figure 1A). The average spatial distances separating the anchor RP23-201H14 and the markers located within the C_H region cluster (h2 and h3) increased as a function of genomic separation (Figures 1B and 1C; Table S1). In pre-pro-B cells, the DNA spanning the *Igh* locus was 100-1000 fold more compacted as compared to linear DNA, which spans about 3.4 nm per ten bp (Table S1). Pro-B cells showed higher compaction values, which were particularly striking in the distal V_H cluster (1284-fold versus 2059-fold between RP23-201H14 and h11) (Table S1). In both pre-pro-B and pro-B cells the spatial distances flattened upon increasing the genomic distance (Figure 1C).

To examine *Igh* topology in nonlymphoid cells, the spatial distances as a function of genomic separation in C57Bl/6 embryonic fibroblasts were determined. In embryonic fibroblasts the average spatial distances separating the anchor and the markers located within the C_H region increased substantially as a function of genomic separation when compared to those observed in pre-pro-B and pro-B cells (Figures S2A and S2B). Thus within this region the chromatin fiber appears to be substantially less compacted as compared to lymphoid cells. These data indicate that the *Igh* locus shows substantial compaction in pre-pro-B cells as compared to nonlymphoid cells, and becomes even more condensed in pro-B cells. Strikingly, however, the spatial distances plateau beyond the D_H elements as a function of increased genomic separation in all three cell-types.

To examine the architecture of a genomic region distinct from that of the *Igh* locus, spatial distances were measured as a function of genomic separation using the RP23-201H14 BAC probe as an anchor and using genomic markers located toward the centromere. The spatial distances again flattened with the topology in pro-B cells being more condensed compared to pre-pro-B cells (Figure S2C). However, for genomic distances larger than 4 Mbp the spatial distances in pre-pro-B and pro-B cells merged

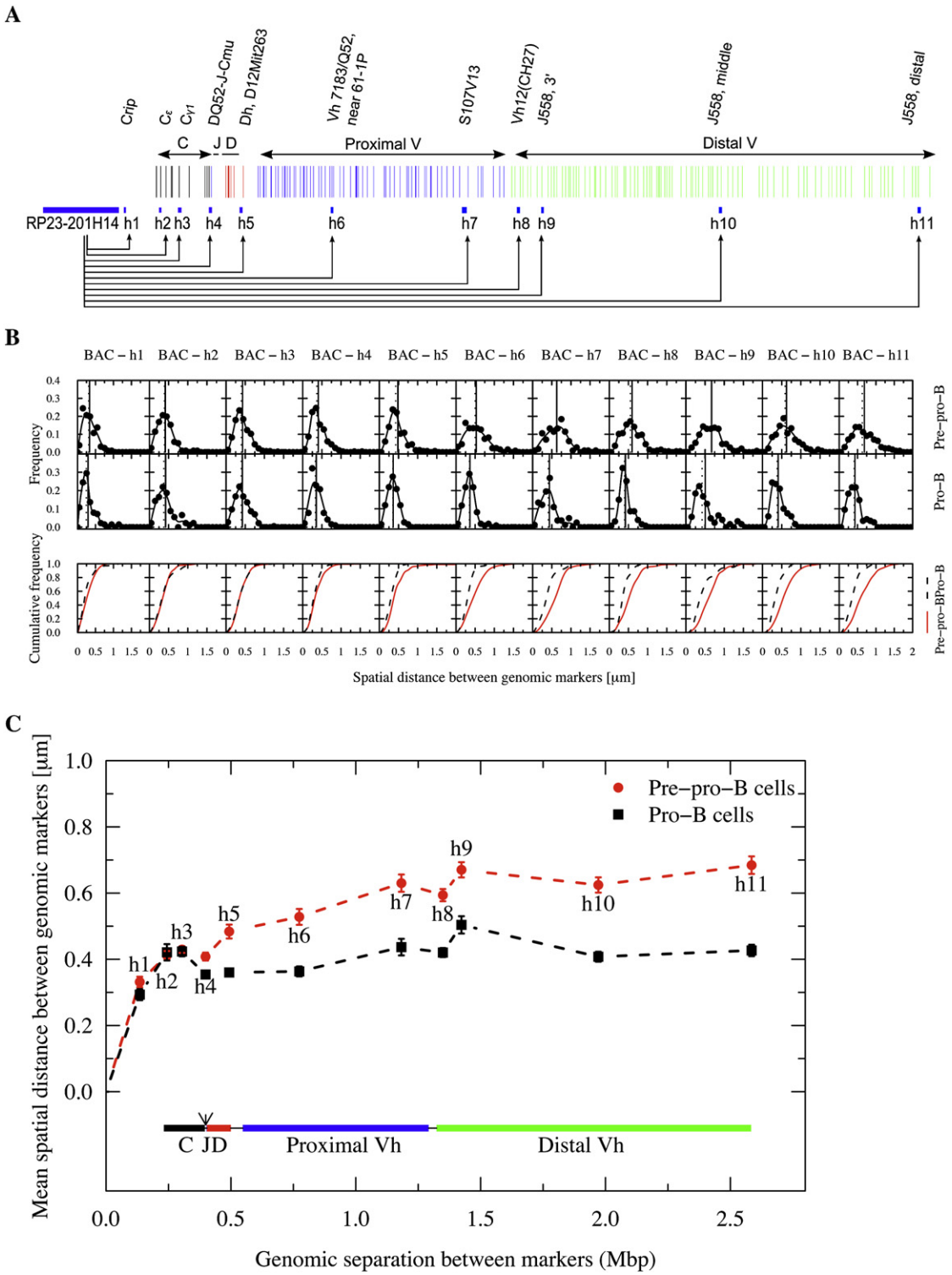

Figure 1. Immunoglobulin Heavy-Chain Locus Spatial Distances and Spatial Distributions as a Function of Genomic Separation in Pre-Pro-B and Pro-B cells

(A) Genomic organization of the *Igh* locus. The anchor and the genomic markers used are indicated.

(B) Frequency plots showing the distribution of spatial distances between the probes and the anchor (RP23-201H14). Cumulative frequency distributions are indicated for both pre-pro-B and pro-B cells.

(C) Average spatial distances were plotted as a function of genomic separation. Distal and proximal variable regions as well as diversity, joining and constant region segments are shown. Bars indicate standard error. The dotted lines only indicate connectivity. The arrow indicates the position of the intronic enhancer.

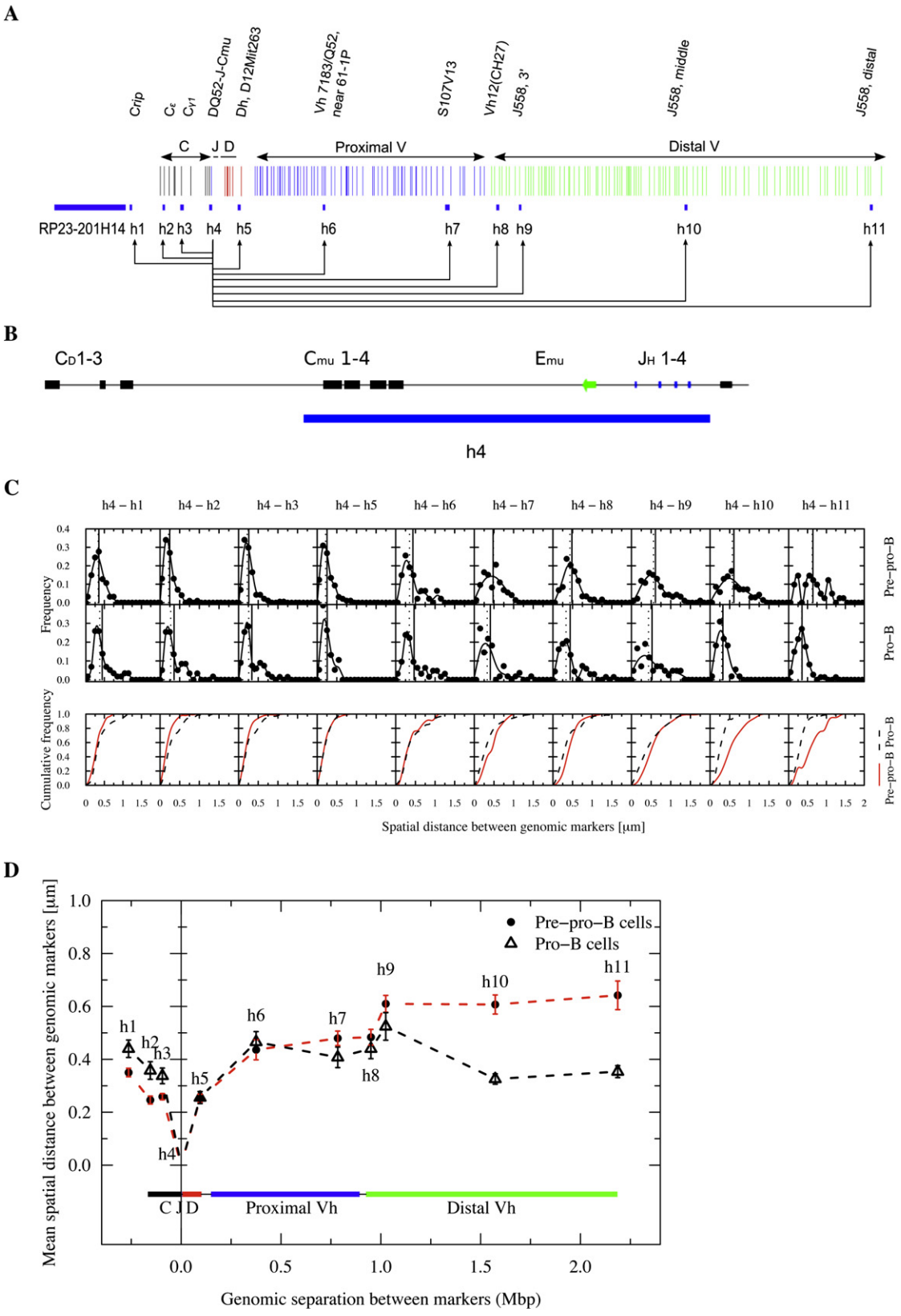
A
Crip
Cε
Cγ1
DQ52-J-Cmu
Dh, D12Mit263
Vh 7183/Q52, near 61-1P
S107V13
Vh12(CH27)
J558, 3'
J558, middle
J558, distal
C
J D
Proximal V
Distal V
RP23-201H14 h1 h2 h3 h4 h5 h6 h7 h8 h9 h10 h11
B
CD1-3
Cmu 1-4
Emu
JH 1-4
h4
C
h4 – h1
h4 – h2
h4 – h3
h4 – h5
h4 – h6
h4 – h7
h4 – h8
h4 – h9
h4 – h10
h4 – h11
Frequency
Pre–pro–B
Pro–B
Cumulative frequency
Spatial distance between genomic markers [μm]
D
Mean spatial distance between genomic markers [μm]
Pre–pro–B cells
Pro–B cells
h1
h2
h3
h4
h5
h6
h7
h8
h9
h10
h11
C J D
Proximal Vh
Distal Vh
Genomic separation between markers (Mbp)

(Figure S2C). In summary, these data indicate: (1) The *Igh* locus assumes different 3D architectures in fibroblasts, pre-pro-B and pro-B cells. (2) The spatial distances plateau as the genomic separation increases.

Long-Range Genomic Separation but Similar Spatial Distances

To determine the spatial distances separating the D_HJ_H elements from the proximal and distal V_H regions, probe h4, containing the D_HJ_H elements, was used as a second anchor (Figures 2A–2D). The average spatial distances between the D_HJ_H elements and the proximal V_H regions (h5 to h8) were similar for pre-pro-B and pro-B cells (Figures 2C and 2D; Table S1). In contrast, the spatial distances separating the distal V_H (h9 to h11) and D_HJ_H regions were substantially reduced in pro-B cells as compared to pre-pro-B cells (Figure 2D). Remarkably, although separated by large genomic distances, the spatial distances separating the proximal and distal V_H regions from the D_HJ_H cluster were similar in pro-B cells (Figure 2D). In fact, the most distal V_H regions were positioned at slightly smaller spatial distances from the D_HJ_H elements than the majority of the proximal V_H regions (Figure 2D).

There are also differences in the spatial distance distributions observed for pre-pro-B and pro-B cells (Table S1). The standard deviations were substantially higher in RAG-deficient pro-B cells for the spatial distances separating the majority of the V_H elements from the D_H-J_H elements (h4-h6, h4-h7, h4-h8, and h4-h9) even though the spatial distances were smaller (Table S1).

Collectively, these data show: (1) During the transition from the pre-pro-B to the pro-B cell stage, the *Igh* locus is remodeled to position the entire set of V_H regions at similar distances to the D_HJ_H elements. (2) The chromatin fiber that contains the proximal V_H, D_H and J_H elements assumes a wider spectrum of configurations in pro-B versus pre-pro-B cells.

Long-Range Genomic Interactions and the Probability of V_H to D_HJ_H Joining

The physical process of DNA recombination requires that the V_H, D_H and J_H segments be mobile, allowing them to interact with each other with detectable frequencies. To assess the probabilities of such encounters, the cumulative frequencies of the spatial distances that separate the V_H regions from the D_HJ_H elements were determined (Figure 2C). The cumulative frequency of a marker indicates the fraction of the alleles in which the marker is within a certain distance from the anchor.

To compare the probabilities of different V_H regions to associate with D_HJ_H elements within the same cell type, the cumulative frequencies were plotted for pre-pro-B and pro-B cells (Figure 2C and S3). As expected, in pre-pro-B cells the probabilities of V_H regions to encounter D_HJ_H elements correlated well with increasing genomic separation (Figure 2C and S3). However, in pro-B cells the cumulative frequencies were clustered at short spatial distances for the majority of the V_H regions (Figure S3). Thus in pro-B cells the probabilities for V_H regions to be localized within close proximity of the D_HJ_H elements are similar regardless of large differences in genomic separation.

The Immunoglobulin Heavy-Chain Topology Cannot Be Described as a Self-Avoiding Random Walk or Worm-like Chain

As a first approach toward elucidating the spectrum of *Igh* topologies, we compared the experimental data with various models of chromatin structure. We found using linear regression that the spatial distance (R) scaled with genomic distance (N) as a power law with exponent ν of 0.25 for pre-pro-B cells and 0.1 for pro-B cells (data not shown). These values differ significantly from that expected of a free random walk (0.5) and a self-avoiding chain ($\sim$0.6) (de Gennes, 1979).

We further examined the scaling property of the probability distribution functions (P(R,N)), by plotting $PN^{3\nu}$ as a function of R/N^{ν} on log-log plots (Figures 3A–3D). If the *Igh* locus configurations can be described as a self-avoiding random walk, then all the data points (distance from either anchor (BAC and h4) to any of the genomic markers) are expected to collapse to a single curve when the exponent ν is chosen to be $\sim$0.6 (de Gennes, 1979). This is clearly not the case for either anchor (BAC and h4) (Figures 3A–3D). Interestingly for values of ν below 0.3 ($\sim$0.1–0.2 for pre-pro-B cells and $\sim$0.1 for pro-B cells), the data points do collapse (Figure S4). However, the interpretation for $\nu < 1/3$ is unclear.

To determine whether the *Igh* topology fits a worm-like chain behavior, the experimental spatial distances as a function of genomic separation were directly compared to the Porod-Kratky chain (see Experimental Procedures for details) (Kratky and Porod, 1949). Different values for the persistence length and chromatin density were chosen that previously were shown to describe the physical properties of the yeast chromatin fiber (Bystricki et al., 2004). However, the spectrum of *Igh* conformations in pre-pro-B cells did not compare well with the worm-like chain, for the different persistence length and chromatin compaction values that were examined (Figures 3E and 3F). Taken together, these data demonstrate that the *Igh* locus topology cannot be described in terms of a self-avoiding random walk or worm-like chain.

Analysis of the *Igh* 3D Architecture by Comparison to Structural Computer Models

To explore the IgH 3D architecture in more detail, computer simulations of potential configurations of chromatin structure were

Figure 2. Immunoglobulin Heavy-Chain Locus Topology in Pro-B Cells Brings Distal V_H Regions and D_HJ_H and Enhancer Elements in Close Spatial Proximity

(A) Genomic organization of the *Igh* locus. The anchor and the genomic markers used are indicated.

(B) Probe h4 contains the J_H segments, the intronic enhancer and C_μ elements.

(C) Frequency plots showing the distribution of spatial distances for each genomic marker from the *Igh* D_H-J_H cluster. Cumulative frequency distributions are indicated for both pre-pro-B and pro-B cells.

(D) Average spatial distances were plotted as a function of genomic separation for each of the probes. Distal and proximal variable regions as well as diversity, joining and constant region segments are shown. Bars indicate standard error. The dotted lines only indicate connectivity. The arrow indicates the position of the intronic enhancer.

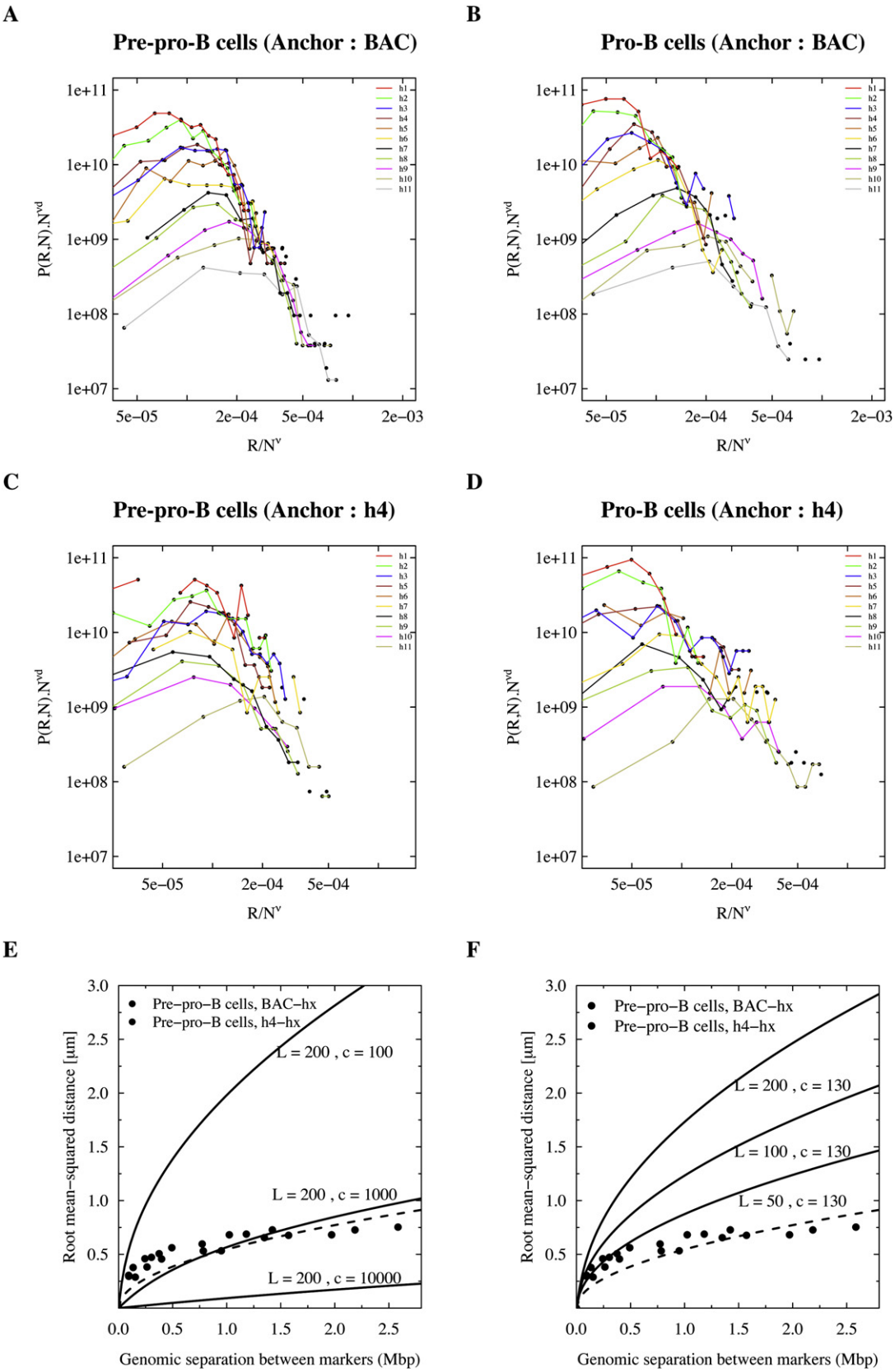
A
Pre-pro-B cells (Anchor : BAC)
B
Pro-B cells (Anchor : BAC)
C
Pre-pro-B cells (Anchor : h4)
D
Pro-B cells (Anchor : h4)
P(R,N).N^vd
R/N^v
1e+11
1e+10
1e+09
1e+08
1e+07
5e−05
2e−04
5e−04
2e−03
h1
h2
h3
h4
h5
h6
h7
h8
h9
h10
h11
E
F
Root mean−squared distance [µm]
Genomic separation between markers (Mbp)
Pre−pro−B cells, BAC−hx
Pre−pro−B cells, h4−hx
L = 200 , c = 100
L = 200 , c = 1000
L = 200 , c = 10000
L = 200 , c = 130
L = 100 , c = 130
L = 50 , c = 130
0.0
0.5
1.0
1.5
2.0
2.5
3.0

performed using Monte-Carlo and Brownian Dynamics methods (Figure 4A) (Knoch, 2002). Two chromatin topologies, the RW/GL and MLS models, were used. In the RW/GL model, the chromatin fiber is organized into large loops (0.5–5.0 Mbp) that are attached to a fixed backbone (Figure 4D). The MLS model implies that the chromatin fiber is organized into rosette-like subcompartments (1–2 Mbp) with smaller loops (60–250 kbp) connected by linkers of variable sizes (60–250 kbp) (Figure 4D).

It is well established that nucleotide content substantially alters the physical properties of the chromatin fiber. However, as a first approach the chromatin fiber was modeled as an elastic homogeneous polymer since it is not known how nucleotide content affects the persistence length of eukaryotic chromatin. To consider both fixed and flexible chromatin architectures, virtual markers were placed in positions that were either dependent or independent of the simulated chromatin architectures (Knoch, 2002) (Figure 4B). Position-dependent spatial distance measurements assume that loops are fixed structures. Hence, spatial distances may differ substantially due to the relative positions of genomic markers with respect to a loop base. The anchor was placed on the base of the loop and virtual distances were measured (Figure 4B; marker 1). The virtual spatial distances were measured from the anchor to other markers in the modeled rosette (red), in the linker (blue), and in the adjacent rosette (green), and then plotted as a function of genomic separation (Figure 4C). This analysis showed the characteristic oscillations of spatial distances as a function of genomic separation consistent with a fixed loop structure localized within a rosette (Figure 4C, dashed lines, and Figure 4E).

Using a position-independent approach, the virtual anchors were placed randomly at different topological positions in the simulated chromatin fiber (Figure 4B; anchors A–F). The average virtual spatial distances, using the RW/GL and MLS models as starting configurations and randomly placed probes, were determined and plotted as a function of genomic separation (see Supplemental Methods for details). As expected, the spatial distances for the RW/GL and MLS models, flattened as the linker sizes were decreased (Figure 4C, solid lines). The simulated data, using the RW/GL model as a starting configuration, did not compare well with the experimental data obtained from the measurements for both pre-pro-B and pro-B cells (Figures 4F and 4G; lines b–h). However, the trend of the spatial distances as a function of genomic distances in pre-pro-B cells agreed well with that predicted by the MLS model (Figures 4F and 4G; compare blue dots and green circles to line A). Thus, in pre-pro-B cells the spatial organization of the *Igh* locus compares well with a topology in which the chromatin fiber is organized into multi-loop containing subcompartments (1 Mbp) connected by 63–126 kbp linkers. In contrast, in pro-B cells the *Igh* fiber showed a substantially more condensed topology than predicted by the MLS model for 126 kbp loops and a linker size of 63 kbp (Figures 4F and 4G; compare pink diamonds and red squares to line A). Collectively, the comparison of the experimental data and the simulations shows that: (1) In pre-pro-B cells, the *Igh* topology agrees well with the MLS model. (2) In pro-B cells the *Igh* locus topology is not consistent with the MLS model in which 1 Mbp compartments are separated by linkers that are similar or larger than 63 kbp.

3D Structure of the Immunoglobulin Heavy-Chain Locus

In order to determine the relative 3D coordinates of the V_H, D_H, J_H and C_H elements within the *Igh* locus, the average spatial distances separating different pairs from the twelve genomic markers were analyzed by trilateration. To obtain the 3D coordinates of genomic markers by trilateration, spatial distances of all the markers from a minimum of four reference probes are needed. Consequently, the spatial distances separating all the probes from each of the three reference probes, BAC RP23-201H14, h3 and h4, were determined (Table S4; see Supplemental Experimental Procedures for details). Instead of using a fourth reference point, additional measurements were made for consecutive probe-pairs. Applying this methodology, the average positions for the genomic markers (BAC, h1–h11) that span the entire *Igh* locus were determined (Table S4). The errors generated by this analysis ranged between 5–100 nm for pro-B cells and 40–150 nm for pre-pro-B cells (Table S5).

In pre-pro-B cells, relatively large spatial distances separated the distal V_H, proximal V_H and C_H regions (Figure 5A; see also Movie S1). The C_H elements were clustered (h2-h4) (Figure 5A; gray objects). Interestingly, the D_H segments (h4 and h5) were positioned away from the majority of the V_H regions (h6-h11) (Figure 5A; red connector). The proximal V_H regions (h5-h8) were located adjacent to the distal portion of the markers that contain D_H elements and were spatially separated from the distal V_H regions (h9-h11) (Figure 5A; green objects; see also Movie S1).

The *Igh* topology in pro-B cells was strikingly different. The pro-B *Igh* locus appeared to have collapsed for the V_H regions that were visualized (Figure 5B; compare Movies S1 and S2). Most remarkable was the merging of the proximal and distal V_H regions (h6-h11) (Figure 5B; see also Movie S2). Whereas in pre-pro-B cells the D_H-J_H elements (h4-h5) were positioned away from the majority of V_H regions, in pro-B cells they were juxtaposed and within relative close proximity to the entire V_H region repertoire (Figure 5B; see also Movie S2).

The data described above bring into question whether the relative average 3D coordinates of the V_H, D_H, J_H and C_H elements reflect the average trajectory taken by the *Igh* fiber in a single B cell. The trilateration analysis considers only two-point

Figure 3. Immunoglobulin Heavy-Chain Topology and Comparison to the Self-Avoiding Random Walk and Worm-like Chain

(A–D) Scaled distributions of spatial distances were plotted for comparison with the self-avoiding walk. A scaling component of v = 0.6 was used. Graphs are shown for both cell types, and with either BAC RP23-201H14 or h4 probes as anchors.

(E) Comparing *Igh* topology to a worm-like chain with a range of chromatin densities (100–10,000 bp/nm) but with a constant persistence length (200 nm). A "least square optimization" analysis is also shown (dotted line).

(F) Spatial distances were plotted as a function of genomic separation and compared with the Porod-Kratky chain with a range in persistence length of 50–200 nm and a constant chromatin density of 130 bp/nm.

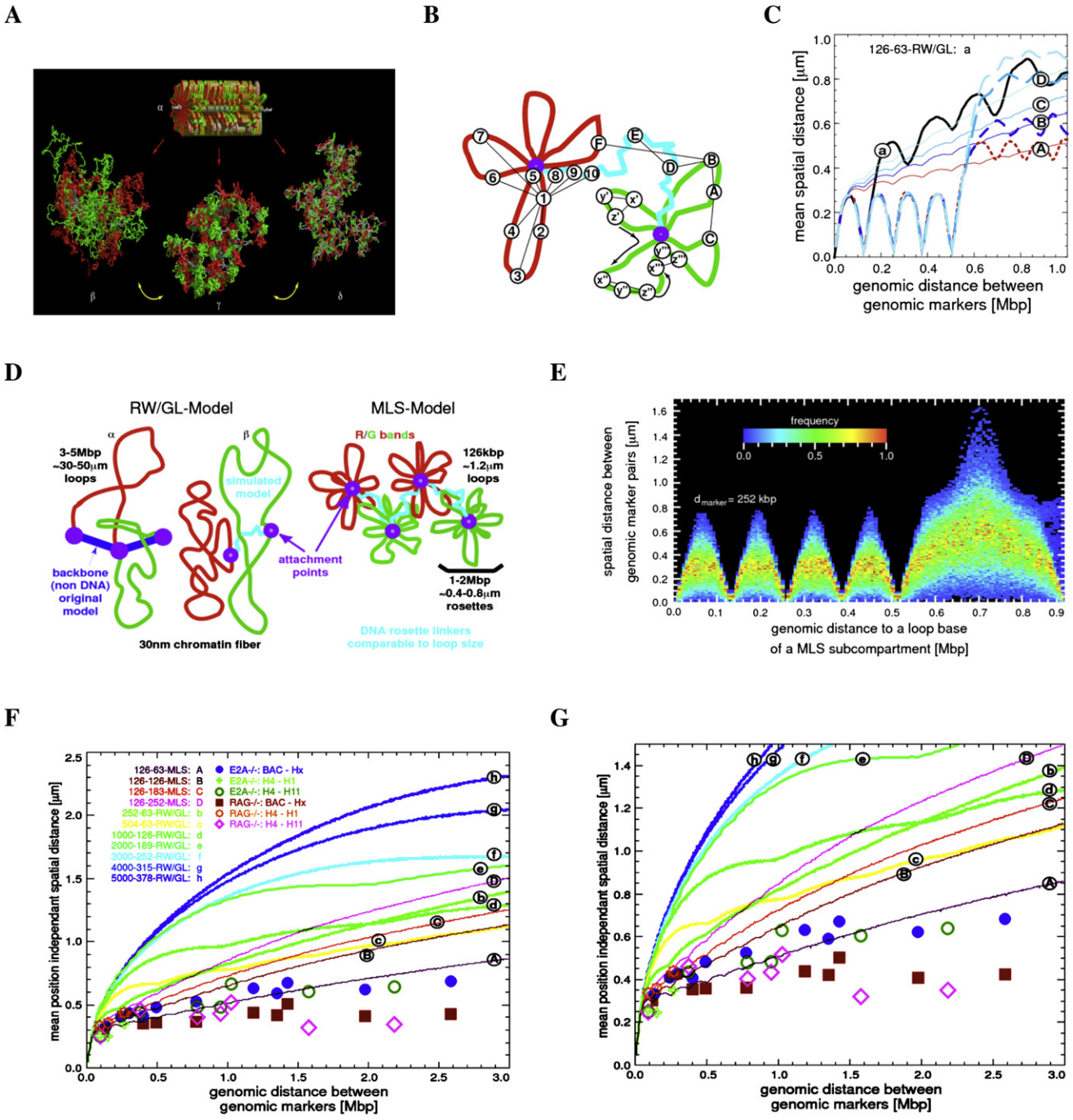

Figure 4. Comparison and Evaluation of Spatial Distances between Genomic Markers in the Immunoglobulin Heavy-Chain Locus by Computer Simulations

(A) Volume rendered images of simulated Random-Walk/Giant-Loop and Multi-Loop-Subcompartment Models. As a starting conformation with the form and size of a metaphase chromosome (top), rosettes were stacked (α). From such a starting configuration, interphase chromosomes in thermodynamic equilibrium, were decondensed by Monte-Carlo and relaxing Brownian Dynamics steps. A volume rendered image of the simulated Random-Walk/Giant-Loop model containing large loops (5 Mbp) is shown (left; β). Note that the large loops do not form distinct structures but intermingle freely (left; β). In contrast, in a volume rendered image of the simulated Multi-Loop-Subcompartment Model, containing 126 kbp sized loops and linkers, the rosettes form distinct chromatin territories in which the loops do not intermingle freely (middle; γ). Also is indicated an image of the simulated RW/GL model containing 126 kbp loops and 63 kbp linkers (right; δ). Note that the small loops do not intermingle freely. Distinct chromatin territories cannot be detected (Knoch, 2003).

(B) Strategy for position-dependent and position-independent virtual spatial distance measurements. For position-dependent virtual distance measurements, the anchor was placed close to the base of the loop (marker 1). The virtual spatial distances were measured from the anchor to other makers in the rosette (1–7) and to a linker (8–10). For position-independent measurements a set of markers separated by the same genomic distance were randomly positioned (x,y,z).

measurements obtained from average distances that were accumulated from large numbers of cells. Two point measurements, however, do not provide insight into the average path taken by the chromatin fiber in a single cell. At least three data points are required. Thus, as a first approach to determine to what degree the trajectory revealed by trilateration reflects the route taken by the *Igh* fiber in single cells, we determined the angular distributions between different combinations of the triple point measurements that were performed. The medians of the experimentally derived angles were then compared to the angles obtained by trilateration. The majority of the median angles observed in pre-pro-B and pro-B cells compared well with those determined by trilateration (Figure S5).

The trilateration analysis also indicated oscillation of spatial distances within the pro-B compartment containing the V_H cluster. For example, h5 is separated by 1.5 Mbp of DNA from h10 but positioned in relatively close spatial proximity (Figure 5). On the other hand, h5 and h6 are in relatively close genomic proximity but separated by a relatively large spatial distance (Figure 5). These observations reveal how the *Igh* topology permits DNA elements that are separated by large genomic distances to be localized in relative close spatial proximity.

We note that although the data points that were analyzed span the entire Ig locus, the number of genomic markers that could be used in this study was restricted. It will be important to provide a higher resolution average trajectory of the *Igh* locus, but this will require a large set of relatively small probes using a strategy recently described for protein folding (Chen et al., 2007). Collectively, these studies show the relative average spatial positions of the V_H, D_H, J_H and C_H elements in both pre-pro-B and pro-B cells. Furthermore, upon commitment to the B cell fate, striking conformational changes in *Igh* topology occur, to allow the entire V_H repertoire encounter D_H elements with relatively high and similar frequencies.

Compartmentalization of the Immunoglobulin Heavy-Chain Locus

To examine whether the clusters visualized by trilateration are localized within distinct subcompartments, we analyzed whether groups of genomic markers located in spatial proximity move coordinately toward or away from the anchor in a single cell (Figure S6A). As an anchor we used BAC RP23-201H14. Triple point spatial distances were derived from single cells separating the anchor and two consecutive probes (h1-h2, h2-h3, h3-h4, h4-h5, h5-h6, h6-h7, h7-h8, h8-h9, h9-h10, and h10-h11). We then computed the group correlation coefficients to determine the degree of coordinated movement. A correlation coefficient of 1 indicates perfectly coordinated positioning of the two markers relative to the anchor. On the other hand, a correlation coefficient of 0 demonstrates a lack of linear correlation in the distances that separate the markers from the anchor in single cells.

There was significant correlation between the spatial distances for the majority of consecutive probes separated from the anchor in pre-pro-B cells (Figure S6A). Two exceptions were notable, markers h1 and h2 as well as h6 and h7 seem to move independently with respect to the BAC RP23-201H14 anchor, suggesting that these markers are located in separate compartments (Figure S6A). Thus, these data suggest that in pre-pro-B cells the *Igh* locus is organized into at least three distinct compartments (BAC-h1; h2-h6; h7-h11). On the other hand, the correlation coefficients for pro-B cells were substantially lower when compared to those of pre-pro-B cells (Figure S6B). Consequently, these data support a pre-pro-B *Igh* configuration in which the position of the markers within a chromatin compartment are relatively fixed and the trajectory of the chromatin fiber within the compartments can be described by a fixed path such as that generated by trilateration whereas the trajectories of the *Igh* fiber in pro-B cells show more flexibility.

If the *Igh* topology were to be organized as compartments in pre-pro-B cells, predicted by the comparison of the experimental and simulated data and the grouping analysis, chromatin territories should be visualized if the entire *Igh* locus were to be fluorescently labeled. Hence, we labeled a set of overlapping BACs that comprise the entire *Igh* locus (Figure 6A). Both pre-pro-B and pro-B cells were hybridized with probes encoding the entire locus and analyzed by epifluorescence microscopy as described above. In pre-pro-B cells 1–3 clusters were visualized whereas in pro-B cells only one cluster was distinguishable (Figures 6B and 6C). Additionally, the linkers connecting the compartments could be visualized (Movies S3–S7).

Statistical Description of Long-Range Genomic Interactions

The data described above show that the *Igh* locus is organized into territories, in which the V_H and J_H-C_H elements are packed at high genomic density in separate compartments. These findings raise the question whether this structure mechanistically permits long-range V_H-D_HJ_H encounters to occur with higher frequencies than would be predicted if the chromatin fiber were not compartmentalized. We assume that close spatial proximity directly relates to the probability of genomic encounters. Thus, we compared the experimental cumulative frequencies obtained

(C) Comparison between simulated position-dependent (dotted lines) and position-independent (solid lines) spatial distances. The curves (A–D) indicate simulated MLS models with 126 kbp loops and different linker sizes. RW/GL is shown for comparison (a). Position-dependent distances (dotted lines) show a stepwise increase in the region where a linker is connecting two chromatin sub-compartments, while position-independent distances (solid lines) do not show the stepwise increase in spatial distances as a function of genomic separation.

(D) Random-Walk Giant Loop and Multi-Loop-Subcompartment Models. α indicates the RW/GL model in which large loops are attached to a non-DNA backbone. β shows the simulated model containing a chromatin linker between loops. MLS model is shown containing 126 kbp loops and linkers with individual rosettes spanning 1–2 Mbp (Knoch, 2003).

(E) The simulated spatial distances as a function of genomic separation are shown for a fixed loop structure. The simulated loop size was 126 kbp. Two virtual genomic markers were chosen that were separated by 252 kbp. The heat map indicates the frequency distribution of simulated spatial distances.

(F and G) Comparison between experimental data and computer simulated data obtained from spatial distance measurements in the *Igh* locus as a function of genomic separation (5.2 kbp steps). Nomenclature is loop size (kbp)-linker size (kbp)-topology. Experimental spatial distance measurements (μm) were plotted as a function of genomic separation (Mbp) for pre-pro-B cells (blue dots and green circles) and pro-B cells (red squares and pink triangles).

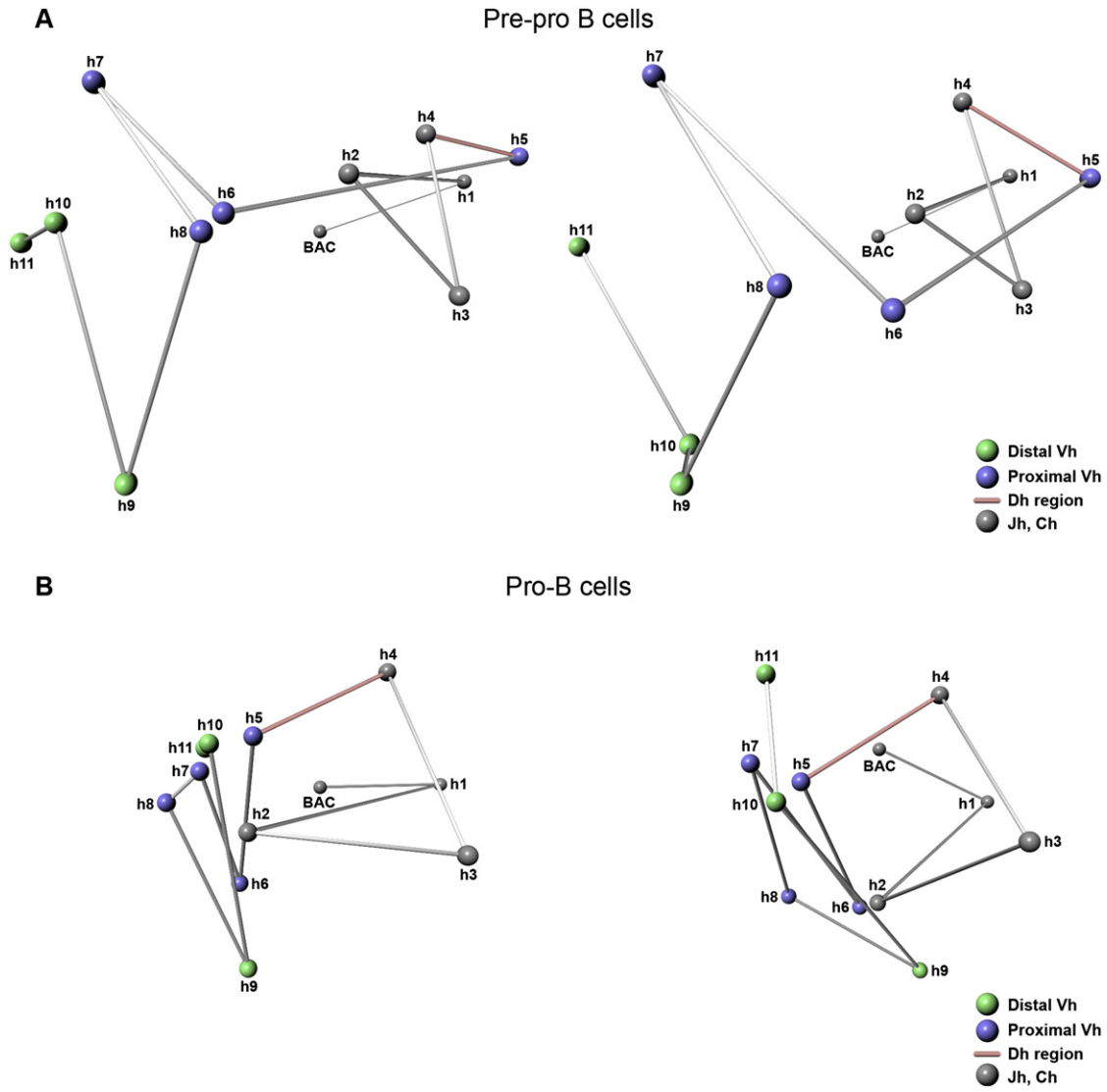

Figure 5. 3D Topology of the Immunoglobulin Heavy-Chain Locus

The 3D topology of the *Igh* locus in pre-pro-B and pro-B cells was resolved using trilateration. The relative positions of 12 genomic markers spanning the entire immunoglobulin heavy-chain locus were computed. Two different views are shown for both cell types.

(A) 3D Topology of the *Igh* locus in pre-pro-B cells.

(B) 3D Topology of the *Igh* locus in pro-B cells. Grey objects indicate C_H regions and the 3′ flanking region of the *Igh* locus. Blue objects indicate proximal V_H regions. Green objects indicate distal V_H regions. Red line indicates the linker connecting the proximal V_H and J_H regions. Linkers are indicated only to show connectivity.

from the spatial distance measurements directly to the cumulative frequency distributions as predicted by a 3D random walk (see Experimental Procedures for details). Interestingly, the theoretical distance distribution for a 3D random walk approached the distance distribution observed for the D_H cluster (Figure 7; h4-h5). These data indicate that the probabilities for D_H elements to be in close proximity to the J_H elements approach those observed for a random walk. In contrast, for larger genomic separations, the theoretical distance distributions did not compare well with the observed spatial distance distribution, consistent with the presence of chromatin territories and spatial confinement (Figure 7; h4-h7, h4-h10 and h4-h11). Consequently, we conclude that it is the *Igh* topology that mechanistically permits long-range genomic interactions to occur in pro-B cells with relatively high frequency.

DISCUSSION

Immunoglobulin Heavy-Chain Locus Topology

How chromosomes are structured in 3D space is largely unknown and only recently data have emerged that have provided insight into the organization of the chromatin fiber in eukaryotic nuclei. Such studies have described the yeast chromatin fiber, in large part, as a worm-like chain (Bystricky et al., 2004). The

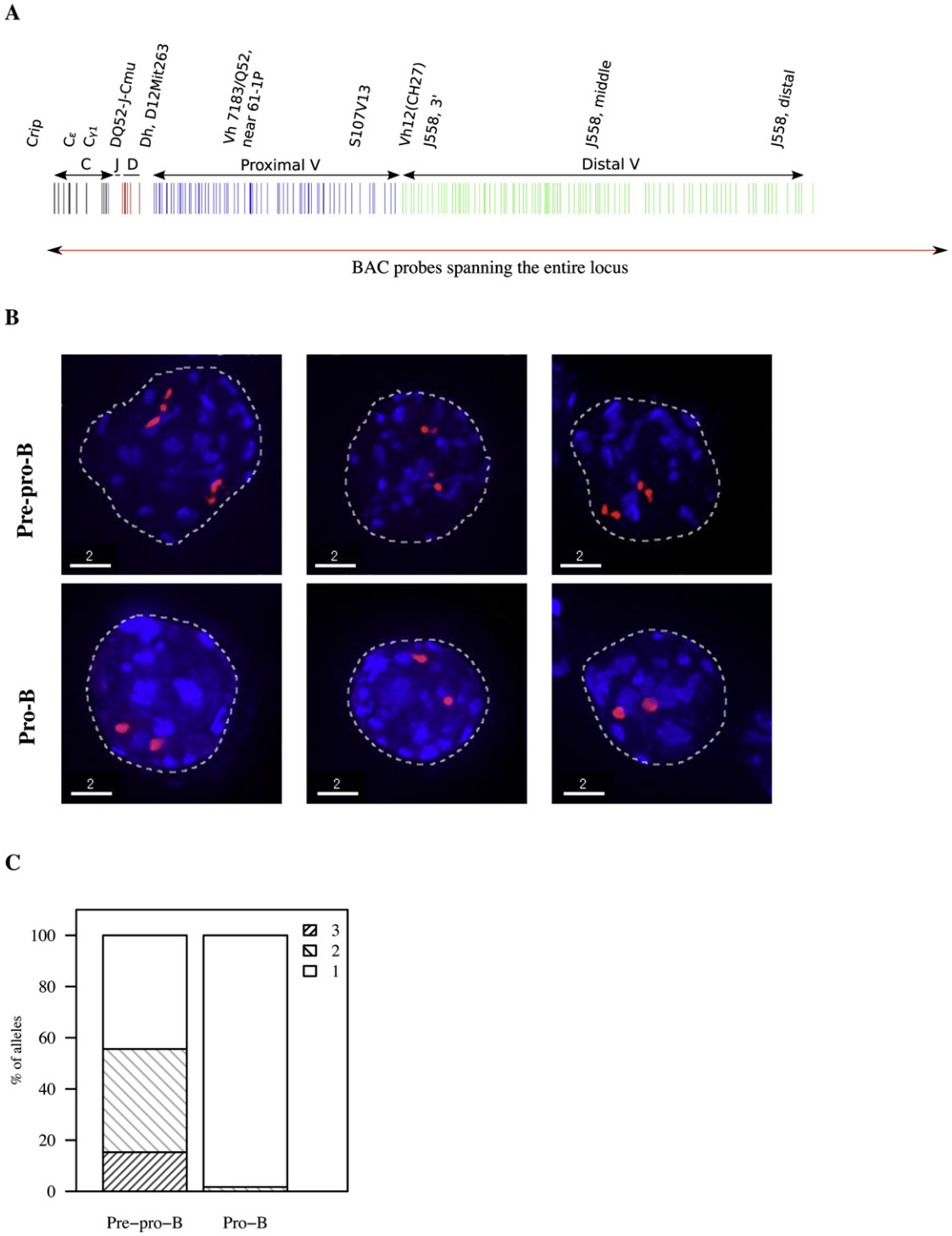

Figure 6. Visualization of the Entire Immunoglobulin Heavy-Chain Locus

(A) *Igh* locus was fluorescently labeled using BACs that span the entire locus.

(B) 3D FISH in nuclei derived from pre-pro-B and pro-B cells using fluorescently labeled BACs that span the entire *Igh* locus. Digitally magnified pictures of the *Igh* locus are shown. BACs (shown in red) were directly labeled with dUTP conjugated to Alexa 568. Nuclei were visualized by DAPI staining.

(C) Fractions of the number of compartments visualized using overlapping set of BAC probes in pre-pro-B and pro-B cells are indicated.

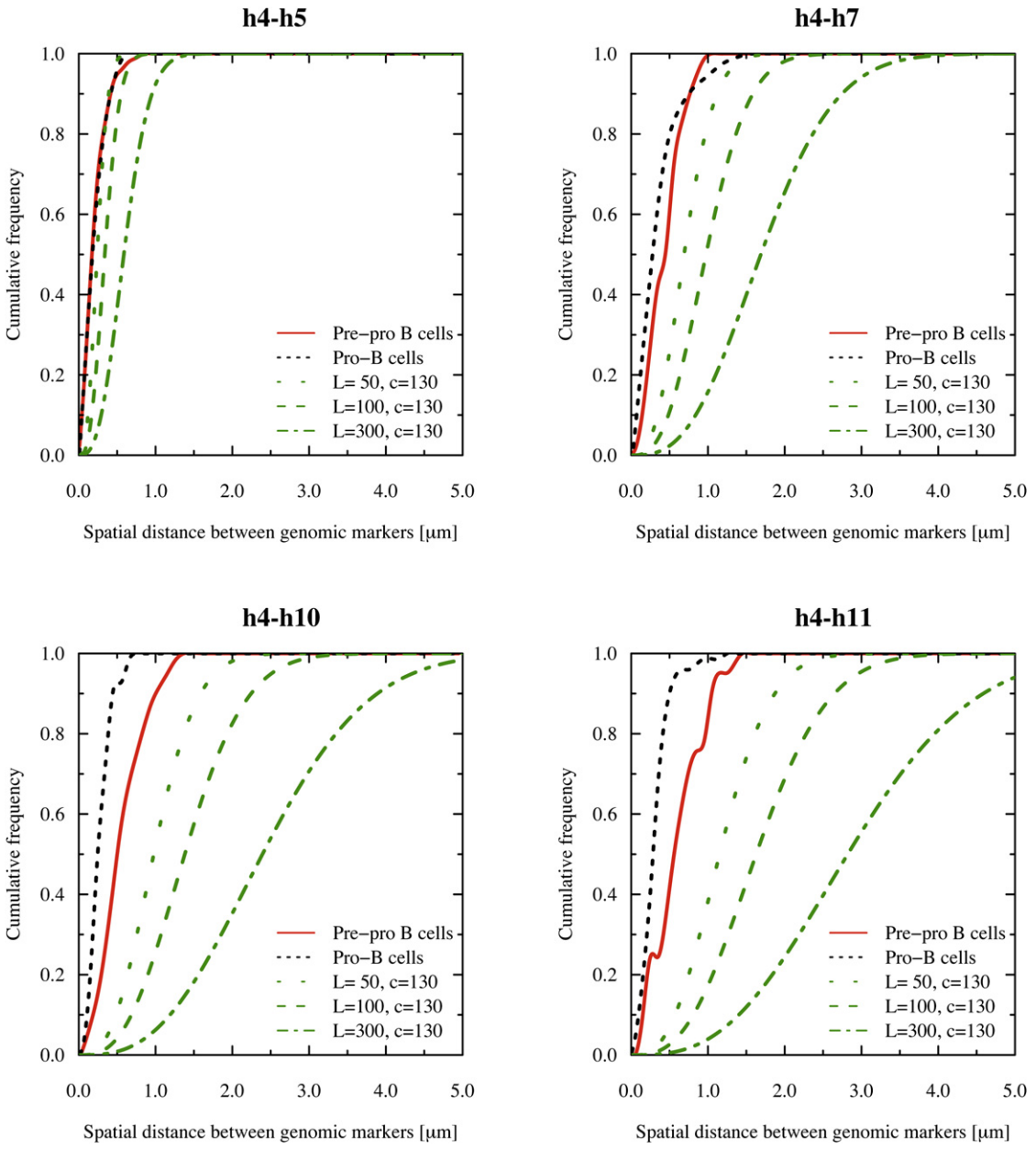

Figure 7. Probabilities of Long-Range Interactions in Pre-pro-B and Pro-B Cells Compared to Those Predicted by a 3D Random Walk

Cumulative frequencies were obtained by accumulating the frequency values corresponding to the spatial distances in intervals of 100 nm using the D_HJ_H elements (probe h4) as an anchor. Cumulative frequency distributions for the random walk were determined for different persistence lengths (see Experimental Procedures). The cumulative frequency distribution for the spatial distance between h4 and h5 is similar for pre-pro-B cells, pro-B cells and for a random walk with a persistence length of 50 nm and chromatin density of 130 bp/nm.

spatial distance distributions observed within the *Igh* locus in B cells, however, are not well fitted by either the self-avoiding or the worm-like chain. A better fit was obtained by comparing the experimental values for those obtained applying Monte-Carlo and Brownian Dynamics methods using the MLS model as a starting configuration. The MLS model assumes the presence of rosettes, spanning about 1–2 Mbp of genomic sequence, connected by linkers of variable sizes (Munkel and Langowski, 1998). In particular, the spatial distributions of the pre-pro-B *Igh* locus topology compared well with the MLS model (126 kbp loops and 63 kbp linkers). Does this comparison imply that the *Igh* pre-pro-B topology is structured as 126 kbp loops? We consider this unlikely but rather suggest that loop size within the compartments varies and determined by proteins associating with the bases of loops, including Pax5, YY1, CTCF and Satb1.

The *Igh* topology in pro-B cells showed a substantial more condensed topology predicted by the modeling of the MLS

configuration for the shortest linker (63 kbp) that was simulated. Since shortening the linker further would essentially merge putative compartments, this latter observation raised the possibility that the *Igh* locus in pro-B cells is organized into one compartment. Indeed group correlation coefficient analysis as well as visualization of the entire *Igh* locus indicated the presence multiple compartments in pre-pro-B cells separated by linkers, whereas only a single compartment was observed in pro-B cells. We note that the data, however, does not rule out the presence of subcompartments in pro-B cells.

The *Igh* topology in nonlymphoid cells, for example, mouse embryonic fibroblasts showed a configuration that is even more decondensed as compared to pre-pro-B cells. However, flattening of the spatial distances as a function of genomic separation was also observed in the *Igh* locus in fibroblasts, indicative of topological confinement as described above for the pre-pro-B and pro-B cell configuration. We note that the *Igh* locus in fibroblasts is located in close proximity of the nuclear membrane, whereas in B-lineage cells it is positioned in more centrally located domains (Kosaki et al., 2001). It is conceivable that the nuclear location of the *Igh* locus affects *Igh* topology. The differences in *Igh* topology in the different cell types are quite remarkable and it will be of interest to determine by trilateration how the *Igh* locus is structured in other cell types as well, including fibroblasts, stem and germ cells.

Immunoglobulin Heavy-Chain Locus Topology and Function

The repositioning of the D_H cluster and the merging of the proximal and distal V_H regions during early B cell development are intriguing. We propose that these conformational changes underpin the mechanism by which a diverse antibody repertoire is established. Although separated by large genomic distances, apart from frequent rearrangements involving the two most proximal V_H regions, Vh81X and VhQ52, little correlation has been observed between V_H region usage and V_H genomic location (Yancopoulos et al., 1984; Malynn et al., 1990; Gu et al., 1991; Love et al., 2000). Thus, V_H regions despite separated by large genomic distances rearrange with similar frequencies.

How do V_H elements separated by large genomic distances find D_HJ_H elements with probabilities that are similar to V_H elements that are localized within close genomic proximity? The trilateration analysis and comparison of experimental and simulated data indicates that it is the folding of the *Igh* fiber that allows a 2 Mbp genomic region to be packed as bundles of loops, allowing the entire V_H region repertoire, regardless of their genomic location, similar access to the D_HJ_H elements.

Long-Range Genomic Interactions

The data also bring into question whether the topology described here is restricted to that of the *Igh* locus, since the *Igh* locus undergoes genomic rearrangement and has special requirements for proximity. We consider this unlikely since the spatial distances also plateau as a function of genomic separation in the centromeric direction away from the *Igh* locus. This region is not undergoing long-range DNA recombination. Why do the spatial distances as a function of genomic separation plateau in a region that is not undergoing antigen receptor assembly? We propose that the chromatin fiber in nonrearranging genomic regions is folded into multi-loop-containing compartments to promote high-density packing and to permit long-range genomic interactions (Cremer and Cremer, 2001). For example, enhancer elements act over large genomic distances (Banerji et al., 1981). Folding of the chromatin fiber into bundles of loops allows such elements to be in close spatial proximity similar as described here for the *Igh* locus. Thus, antigen receptor genes may simply have utilized this topology to allow large numbers of V_H elements to encounter D_HJ_H or J_H elements with relatively high and similar frequencies. We suggest that enhancer and promoter elements use a similar strategy to interact over large genomic distances.

Spatial Distributions and Immunoglobulin Heavy-Chain Locus Rearrangement

In addition to the large conformational changes that seem to accompany early B cell development, we noted changes in the spatial distributions in pre-pro-B versus pro-B cells. Specifically, the standard deviations in spatial distances using the D_H elements (h4) as an anchor were substantially larger in pro-B cells even though the mean spatial distances were smaller. Why is there a wider distribution of configurations in pro-B versus pre-pro-B cells? We suggest that the larger variation reflects an *Igh* topology in pro-B cells that is less confined or fixed as compared to pre-pro-B cells and that these differences in the range of conformations reflect the requirement for the *Igh* fiber in pro-B cells to be flexible in order for the large number of V_H regions that span over 2 Mbp of genomic distance to encounter D_H elements with similar probabilities. Thus we propose that both the average spatial positions as well as the spectrum of conformations change during early B cell development to permit V_H regions scattered over a large genomic region to rearrange with frequencies that seem independent of genomic location.

Conclusion

Here, we have used geometry to provide a statistical representation of the *Igh* locus topology. We demonstrate how *Igh* structure permits close encounters between V_H and D_H elements separated by large genomic distances with relatively high probability. We propose that the topology described here is not restricted to that of antigen receptor loci but rather is a general feature of eukaryotic chromatin to promote long-range genomic interactions including promoter and enhancer regulatory elements.

EXPERIMENTAL PROCEDURES

Mice and Cell Culture

All mice used were maintained in a C57BL/6 background. $Rag2^{-/-}$ pro-B cells and $E2A^{-/-}$ hematopoietic progenitors were isolated and grown as described previously (Ikawa et al., 2004; Sayegh et al., 2005). The E2A-deficient and Rag2-deficient targeted mutations were originally engineered in R9 ES cells and subsequently backcrossed on a C57BL/6 background. Since the genomic organization of the *Igh* locus differs substantially between C57BL/6 and 129 mice strains, genomic DNA was isolated from E2A deficient pre-pro-B and RAG2-deficient pro-B cells to determine their origins. PCR analysis at four polymorphic sites, localized throughout the *Igh* locus, confirmed that in both cell types the *Igh* locus is derived from C57BL/6 (R.R., data not shown).

Cloning and Labeling of 10 kb Probes

To identify unique DNA sequences within the *Igh* locus, a percentage identity plot of the *Igh* locus was generated. Eleven unique 10 kbp DNA segments, i.e., regions that were not duplicated within the *Igh* locus and showed minimal genomic repeats, were identified using a percentage identity plot. PCR primers were designed for these regions and long-range PCR (Eppendorf) was used to amplify the 10 kb stretches. PCR products were cloned into the pGEMTEasy vector system (Promega). The sequences of the clones were confirmed by restriction mapping and by DNA sequencing. DNA probes were labeled with aminoallyl-dUTP (ARES labeling kits, Invitrogen) by nick-translation (Roche). One μg of DNA was labeled in a 20 μl reaction for 3 hr and 45 min. Nick-translated 10 kbp products were size selected on a 0.6% agarose gel and 10–500 bp fragments were purified using a QIAGEN gel extraction kits. Aminoallyl-modified DNA was fluorescently labeled with succinimidyl ester derivatives of Alexa fluorochromes (Alexa 488, 594, or 647).

The Self-Avoiding Chain and Kratky-Porod Analytical Description of a Polymer

The probability density between genomic markers can be determined as:

$$P(\mathbf{R}, a) = \left(\frac{3c}{2\pi da}\right)^{\frac{3}{2}} e^{-\frac{3cR^2}{2da}} \qquad \text{Equation 1}$$

"a" is the Kuhn length of DNA (nm) and "c" is the DNA mass density (bp/nm) (Grosberg and Khokhlov, 1997). The cumulative frequency distribution F(R) is given by:

$$\int_0^R \left(\frac{3c}{2\pi da}\right)^{\frac{3}{2}} e^{-\frac{3cR^2}{2da}} 4\pi R^2 dR. \qquad \text{Equation 2}$$

The distribution of spatial distances as a function of genomic separation for the self-avoiding chain are described as follows:

$$P(R, N) = N^{-\nu d} f\left(\frac{R}{N^{\nu}}\right) \qquad \text{Equation 3}$$

R, spatial distances separating genomic markers; N, genomic separation between the markers; P, frequency value of the spatial distance R for markers separated by N base-pairs; d, number of dimension in which the distances have been measured. Here, d = 3; ν = 0.6 for self-avoiding random walks.

$$f(x) = x^{g} \text{ for } x << 1 \qquad \text{Equation 4}$$

$$f(x) = e^{-x^{\delta}} \text{ for } x >> 1. \qquad \text{Equation 5}$$

For a self-avoiding random walk, the constants g and δ are as follows: g = 0.67 ± 0.3 and δ = 2.5.

The Kratky-Porod description of a semiflexible polymer was used to compare the experimental data to that of the worm-like chain: (Kratky and Porod, 1949):

$$\langle R^2 \rangle = 2 \times L^2 \times \left(\frac{d}{cL} - 1 + e^{-\frac{d}{cL}}\right) \qquad \text{Equation 6}$$

where R is the physical distance separating two genetic markers (nm), d is the genomic separation between genetic markers (bp), c is the DNA mass density (bp/nm), and L is the persistence length (nm).

The cumulative frequencies were determined for different persistence lengths and compared with the experimental data. For theoretic spatial distances and frequency distributions, a mass density of 130 bp/nm was used (Bystricky et al., 2004). The experimental frequency distributions were generated after binning 100 nm spatial distances.

SUPPLEMENTAL DATA

Supplemental Data include Supplemental Experimental Procedures, six figures, five tables, and seven movies and can be found with this article online at http://www.cell.com/cgi/content/full/133/2/265/DC1/.

ACKNOWLEDGMENTS

We thank Douglas Forbes and Peter Geiduschek for careful reading and editing of the manuscript; Terry Hwa for help with modeling the self-avoiding chain, suggesting triple point measurements and group correlation coefficient analyses, and for stimulating discussions; and Rob Phillips for stimulating discussions during the initial phase of these studies. We thank the UCSD Microscopy and Imaging Facility for support. T.A.K. thanks the High-Performance Computing Center Stuttgart (HLRS; grant HumNuc), the Supercomputing Center Karlsruhe (SCC; grant ChromDyn), the Computing Facility of the German Cancer Research Center (DKFZ), the Bundesministerium für Bildung und Forschung (BMBF) under grant #01 KW 9602/2 (German Human Genome Project) and under grant 01AK803A (German MediGRID), and the German Cancer Research Center (DKFZ). M.C.v.Z. was supported by a fellowship from the Ter Meulen Fund–Royal Netherlands Academy of Arts and Sciences. S.C. acknowledges the support by Core Grant (Cooperative Agreement No. 05253071) and a Cooperative Support Agreement (CSA 0438741). This study was supported by the National Institutes of Health (S.J., M.P., M.C.v.Z., R.R., and C.M.).

Received: May 27, 2007
Revised: January 4, 2008
Accepted: March 16, 2008
Published: April 17, 2008

REFERENCES

Alt, F.W., Yancopoulos, G.D., Blackwell, T.K., Wood, C., Thomas, E., Boss, M., Coffman, N., Rosenberg, N., Tonegawa, S., and Baltimore, D. (1984). Ordered rearrangement of immunoglobulin heavy chain variable region segments. EMBO J. *3*, 1209–1219.

Banerji, J., Rusconi, S., and Schaffner, W. (1981). Expression of a beta-globin gene is enhanced by remote SV40 DNA sequences. Cell *27*, 299–308.

Bover, T. (1909). Die Blastomerenkerne von Ascaris meglocephala und die Theorie der Chromosomenindividualitaet. Archiv. für Zellforschung *3*, 181–268.

Brodeur, P.H., and Riblet, R. (1984). The immunoglobulin heavy chain variable region (Igh-V) locus in the mouse. One hundred Igh-V genes comprise seven families of homologous genes. Eur. J. Immunol. *14*, 922–930.

Bystricky, K., Heun, P., Gehlen, L., Langowski, J., and Gasser, S.M. (2004). Long-range compaction and flexibility of interphase chromatin in budding yeast analyzed by high-resolution imaging techniques. Proc. Natl. Acad. Sci. USA *101*, 16495–16500.

Carter, D., Chakalova, L., Osborne, C.S., Dai, Y.F., and Fraser, P. (2002). Long-range chromatin regulatory interactions in vivo. Nat. Genet. *32*, 623–626.

Chen, Y., Ding, F., and Dokholyan, N.C. (2007). Fidelity of the protein structure reconstruction from inter-residue proximity constraints. J. Phys. Chem. *111*, 7432–7438.

Cremer, T., and Cremer, C. (2001). Chromosome territories, nuclear architecture and gene regulatin in mammalian cells. Nat. Rev. Genet. *2*, 292–301.

de Gennes, P.G. (1979). Scaling concepts in polymer physics (Cornell University Press).

Eivazova, E.R., and Aune, T.M. (2004). Dynamic alteratins in the conformation of the Ifn gene region during T helper cell differentiation. Proc. Natl. Acad. USA *101*, 251–256.

Fuxa, M., Skok, J., Souabni, A., Salvagiotto, G., Roldan, E., and Busslinger, M. (2004). Pax5 induces V-DJ rearrangements and locus contraction of the immunoglobulin heavy-chain gene. Genes Dev. *18*, 411–422.

Grosberg, A.Y., and Khokhlov, A.R. (1997). Giant Molecules (Academic Press), pp. 78–79.

Gu, H., Tarlington, D., Muller, W., Rajewsky, K., and Forster, I. (1991). Most peripheral B cells in mice are ligand selected. J. Exp. Med. *173*, 1357–1371.

Herendeen, D.R., Kassavetis, G.A., and Geiduschek, E.P. (1992). A transcriptional enhancer whose function imposes a requirement that proteins track along DNA. Science *256*, 1298–1303.

Jung, D., Gillourakis, C., Mostoslavsky, R., and Alt, F.W. (2006). Mechanism and control of V(D)J recombination at the immunoglobulin heavy chain gene. Annu. Rev. Immunol. *24*, 541–570.

Ikawa, T., Kawamoto, H., Wright, L.Y., and Murre, C. (2004). Long-term cultured E2A-deficient hematopoietic progenitor cells are pluripotent. Immunity *20*, 349–360.

Knoch, T.A., Münkel, C., and Langowski, J. (2000). Three-dimensional organization of chromosome territories in the human interphase nucleus. In High Performance Computing in Science and Engineering 1999, W. Jäger and E. Krause, eds. (Berlin-Heidelberg-N.Y.: Springer).

Knoch, T.A. (2002). Approaching the Three-Dimensional Organization of the Human Genome: Structural-, Scaling- and Dynamic-Properties in the Simulation of Interphase Chromosomes and Cell Nuclei, Long-Range Correlations in Complete Genomes, In Vivo Quantification of the Chromatin Distribution, Construct Conversions in Simultaneous Co-Transfections (Mannheim, Germany: TAK Press).

Knoch, T.A. (2003). Towards a Hollistic Understanding of the Human Genome by Determination and Integration of Its Sequential and Three-Dimensional Organization. In High Performance Computing in Science and Engineering 2002, W. Krause and E. Jäger, eds. (Berlin-Heidelberg-N.Y.: Springer).

Kosak, S.T., Skok, J.A., Medina, K.L., Riblet, R., Beau, M.M.L., Fisher, A.G., and Singh, H. (2002). Subnuclear compartmentalization of immunoglobulin loci during lymphocyte development. Science *296*, 158–162.

Kratky, O., and Porod, G. (1949). Röntgenuntersuchung gelöster Fadenmoleküle. Rec. Trav. Chim Pays-Bas *68*, 1106–1133.

Love, V., Lugo, G., Merz, D., and Feeney, A.J. (2000). Individual Vh promoters vary in strength, but the frequency of rearrangement of those Vh genes does not correlate with promoter strength nor enhancer-independence. Mol. Immunol. *37*, 29–36.

Malynn, B.A., Yancopoulos, G.D., Barth, J.E., Bona, C.A., and Alt, F.W. (1990). Biased expression of JH-proximal Vh genes occurs in the newly generated repertoire of neonatal and adult mice. J. Exp. Med. *171*, 843–859.

Münkel, C., and Langowski, J. (1998). Chromosome structure described by a polymer model. Phys. Rev. E Stat. Phys. Plasmas Fluids Relat. Interdiscip. Topics *57*(5B), 5888–5896.

Okada, T.A., and Commings, D.E. (1979). Higher order structure of chromosomes. Chromosoma *72*, 1–14.

Paulson, J.R., and Laemmli, U.K. (1977). The structure of histone depleted metaphase chromosomes. Cell *12*, 817–828.

Paulson, J.R. (1988). Scaffolding and radial loops: the structural organization of metaphase chromosomes. Chromosomes and Chromatin 3 (Boca Raton, Florida: CRC Press), pp. 3–36.

Pienta, K.J., and Coffey, D.S. (1984). A structural analysis of the nuclear matrix and DNA loops in the organization of the nucleus and chromosome. J. Cell Sci. *Suppl. 1*, 123–135.

Rabl, C. (1885). Über Zellteilung. Morphologisches Jahrbuch *10*, 214–330.

Roldan, E., Fuxa, M., Chong, W., Martinez, D., Novatchkova, M., Busslinger, M., and Skok, J. (2005). Locus 'decontraction' and centromeric recruitment contribute to allelic exclusion of the immunoglobulin heavy-chain gene. Nat. Immunol. *6*, 31–41.

Rombel, I., North, A., Hwag, I., Wyman, C., and Kustu, S. (1998). The bacterial enhancer-binding protein Ntrc as a molecular machine. Cold Spring Harb. Symp. Quant. Biol. *63*, 157–166.

Sachs, R.K., van den Engh, G., Trask, B., Yokota, H., and Hearst, J.E. (1995). A random-walk/giant-loop model for interphase chromosomes. Proc. Natl. Acad. Sci. USA *92*, 2710–2714.

Sayegh, C., Jhunjhunwala, S., Riblet, R., and Murre, C. (2005). Visualization of looping involving the immunoglobulin heavy-chain locus in developing B cells. Genes Dev. *19*, 322–327.

Schatz, D.G., and Spanopoulou, E. (2005). Biochemistry of V(D)J recombination. Curr. Top. Microbiol. Immunol. *290*, 49–85.

Solovei, I., Cavallo, A., Schermelleh, L., Jaunin, F., Scasselati, C., Cmarko, D., Cremer, C., Fakan, S., and Cremer, T. (2002). Spatial preservation of nuclear chromatin architecture during three-dimensional fluorescence in situ hybridization (3D-FISH). Exp. Cell Res. *276*, 10–23.

Spilianakis, C.G., and Flavell, R.A. (2004). Long-range intrachromosomal interactions in the T helper type 2 cytokine locus. Nat. Immunol. *5*, 1017–1027.

Tolhuis, B., Palstra, R.J., Splinter, E., Grosveld, F., and de Laat, W. (2002). Looping and interaction between hypersensitive sites in the active β-globin locus. Mol. Cell *10*, 1453–1465.

Trask, B.J., Massa, H., Kenwrick, S., and Gitschier, J. (1991). Mapping of human chromosome Xq28 by two-colour fluorescence in situ hybridization of DNA sequences to interphase cell nuclei. Am. J. Hum. Genet. *48*, 1–15.

Trask, B.J., Allen, S., Massa, H., Fertitta, A., Sachs, R., van den Engt, G., and Wu, M. (1993). Studies of metaphase and interphase chromosomes using fluorescence in situ hybridisation of DNA sequences to interphase cell nuclei. Am. J. Hum. Genet. *48*, 1–15.

Warrington, J.A., and Bengtsson, U. (1994). High-resolution physical mapping of human 5q31-q33 using three methods: radiation hybrid mapping, interphase fluorescence *in situ* hybridization, and pulsed-field gel electrophoresis. Genomics *24*, 395–398.

Yancopoulos, G.D., Desiderio, S.V., Paskind, M., Kearney, J.F., Baltimore, D., and Alt, F.W. (1984). Preferential utilization of the most JH-proximal VH gene segments in pre-B-cell lines. Nature *31*, 727–733.

Yokota, H., Engh, G.v.d., Hearst, J.E., Sachs, R.K., and Trask, B.J. (1995). Evidence for the organization of chromatin in megabase pair-sized loops arranged along a random walk path in the human G0/G1 interphase nucleus. J. Cell Biol. *130*, 1239–1249.